ADVANCED MATERIALS INTERFACES
www.advmatinterfaces.de

Biphasic Porous Structures formed by Monomer/Water Interface Stabilization with Colloidal Nanoparticles

*Fabio Pizzetti, Arianna Rossetti, Alessandro Marchetti, Franca Castiglione, Valeria Vanoli, Elena Coste, Valeria Veneruso, Pietro Veglianese, Alessandro Sacchetti, Alberto Cingolani, and Filippo Rossi**

Bicontinuous jammed emulsions (known as bijels) are Pickering emulsions where oil and water are both continuous phases. These interconnected structures, stabilized by colloidal nanoparticles at the oil–water interface, have been used in a wide range of applications. Among these, catalysis and encapsulation of solutes has showed promising potential, but the low mechanical properties of the systems limit their use. Here it is proposed that the use of a hydrophobic monomer able to polymerize in bulk and form a biphasic porous structure with polymer and water as immiscible phases. The final system is stabilized by colloidal nanoparticles made of hydroxyapatite, and the system's ability to release both hydrophilic and hydrophobic drugs has been demonstrated. The strategy has been proven to be highly versatile and may be tuned with a diversity of monomers and nanoparticles to satisfy specific industrial and medical needs.

1. Introduction

Bijels are a particular type of Pickering emulsions where both phases (oil and water) are present in a comparable amount.[1–4] In specific conditions this leads to the formation of a bicontinuous porous interpenetrating structure stabilized by colloidal nanoparticles at the interface. Without nanoparticles a macroscopic phase separation would occur in the system and the two phases would settle depending on their densities.[5,6] The first procedures for Bijels production was demonstrated in the early 2000s. The first experimentally successful method was the so called thermal spinodal decomposition.[7] In 2015 Haase and coworkers improved this method developing a way to cause the spinodal decomposition relying on the removal of a solvent from a ternary mixture.[8] In this case two immiscible liquids are mixed together with a solvent which has the ability to let them become mutually soluble. The so-created mixture is injected into a continuous phase able to extract the solvent, whose abrupt removal induces the spinodal decomposition of the two remaining fluids. More recently, Clegg research group has defined a simpler and quicker production protocol involving just a direct mixing between the components involved.[9] Following this strategy colloidal nanoparticles dispersed into two immiscible fluids and some surfactants are required. In this way it is possible to favor different local curvatures of the interfacial surface and to stabilize the structure. Differently from the spinodal decomposition, the bijel here is formed through the application of high shear rates and therefore, during the initial stages, droplets of the binary mixture are generated. Once the shear is removed, the coarsening process starts trapping the particles[1] at the interfaces until the coalescence is arrested. At the same time, the surfactants impose the local curvature of the liquid–liquid contact surface, helping in the formation of the characteristic bicontinuous architecture. More recently Huang et al.[1,2,10] simplified the production method using only a simple vortex mixing. To do so they employed a combination of different molecular weight surfactants to stabilize different local curvatures to the interface between the two liquid phases.

In this case, the only necessary condition to form a bijel is the use of a mixture of polymers with different molecular weights and a sufficiently high concentration of particles to form a bicontinuous interfacially jammed emulsion gel. In the latest years, bijels has showed promising applications in many industrial fields like batteries, fuel cells and many other fields in which a multiphasic material with controlled structure is of any interest.[11] From a medical perspective the main advantage in using bijels reside in the possibility to obtain a system able

F. Pizzetti, A. Rossetti, A. Marchetti, F. Castiglione, V. Vanoli, E. Coste, A. Sacchetti, F. Rossi
Department of Chemistry
Materials and Chemical Engineering "Giulio Natta"
Politecnico di Milano
via Mancinelli 7, Milano 20131, Italy
E-mail: filippo.rossi@polimi.it

V. Veneruso, P. Veglianese
Department of Neuroscience
Istituto di Ricerche Farmacologiche Mario Negri IRCCS
via La Masa 19, Milano 20156, Italy

A. Cingolani
Department of Chemistry and Applied Biosciences
Institute for Chemical and Bioengineering
ETH Zurich
Vladimir-Prelog Weg 1–5/10, Zurich 8093, Switzerland

The ORCID identification number(s) for the author(s) of this article can be found under https://doi.org/10.1002/admi.202100991.

DOI: 10.1002/admi.202100991

to deliver both hydrophilic and hydrophobic drugs simultaneously following the multidrug delivery strategy.[12,13]

It is indeed well-known that recent progress has led to a paradigm shift in many therapies, like cancer and neurodegenerative diseases, from "one-drug-one-target" to "combination of drugs-multitarget" approaches with the final aim to overcome several therapeutic challenges clinicians are facing today.[12,14] Up to now hydrophobic drugs can be loaded in hydrogels by functionalizing their networks with hydrophobic domains like cyclodextrin or micelles.[15] This approach presents some drawbacks like the low amount of hydrophobic solute that can be loaded,[16] limiting the application to only drugs that exhibits high therapeutic activity even at low concentrations. Furthermore, Bijels can help overcome one of the main problems of nanomedicine: the uncontrolled distribution of nanoparticles though the body.[17] This as one of bijels' peculiarities is the possibility to maintain *in loco* colloidal nanoparticles because they stabilize the system and are entrapped within its structure. Nowadays the main limit to bijel's applications in biomedical field resides in the necessity of high amount of surfactant molecules and inadequate final mechanical properties.[6,18] In the present work we describe a new class of biphasic porous structures that can be easy produced, without surfactants and with improved mechanical properties.

2. Results and Discussion

To address these problems we propose the use a biocompatible hydrophobic monomer that can polymerize in bulk conditions during biphasic porous structure formation. Here we propose the use of e-caprolactone (CL) as oil phase that, together with biocompatible initiator (ethanol) and catalyst (triazabicyclodecene, TBD),[19] undergoes ring-opening polymerization forming a polymer that is hydrophobic as well.

The water phase is constituted by aqueous solution of rod-shaped hydroxyapatite (HA) nanoparticles synthesized following previous protocols, whose nature was determined through X-ray powder diffraction (details and characterization in the Supporting Information). The procedure developed for the formation of biphasic porous structures is illustrated in **Figure 1**. After several tests (for details refer to the Supporting Information) we decided to use a multireax tube shaker (Figure 1a–e). Initially we introduced CL, EtOH and TBD with consequent polymerization at room temperature (shaking at 1000 rpm for 8 min). Then we injected HA NPs (concentration = 20 mg mL^{-1}) dissolved in water, before the system was subjected to additional shaking at 1700 rpm for 40 s, followed by 5 min of shaking at 1000 rpm. At the end the material obtained was removed from the tube without any loss of water (Figure 1f) demonstrating high stability at 37 °C (Supporting Information).

Temperature, shaking time, NPs concentration and injection time were optimized to obtain only partial polymerization. A too early injection of water/NPs will lead to phase separation between monomer (not able to polymerize) and water. On the contrary a too late injection time will cause phase separation between the polymer already formed and the water phase. The results from the parameter optimization is reported in the Supporting information. The two phases used constitute a biphasic porous structure as schematized in **Figure 2**a. The final material

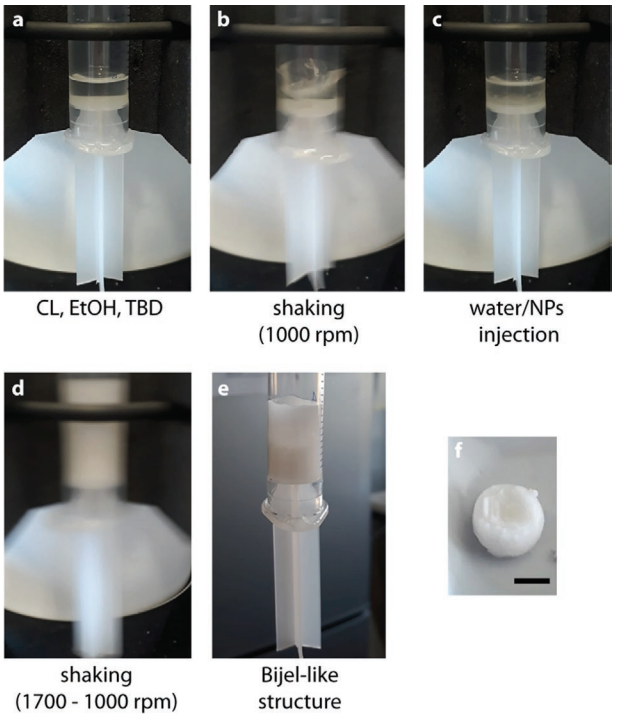

Figure 1. Photographs of the steps used for biphasic porous structures (bijel-like structure) production using a multi reax tube shaker. a) oil phase, b) first shaking where polymerization starts, c) injection of water/NPs solution, d) second shaking, e) obtainment of biphasic porous structure visible in f), without water loss. Scale bar = 0.5 cm.

is presented in Figure 2b. The fact that all the water from the production procedure is entrapped in the polymeric network of the sample highlight the absence of phase separation.

From FTIR spectrum (Figure 2c) of the biphasic porous structures both signals typical of polycaprolactone (PCL) and HA NPs are observable also after repeated washing cycles. For PCL, the absorption band at 2940 cm^{-1} is assigned to the C–H hydroxyl groups asymmetric stretching. The band at 2860 cm^{-1} is assigned to C-H hydroxyl groups symmetric stretching. The absorption band at 1722 cm^{-1} is assigned to –C=O stretching vibrations of the ester carbonyl group. The absorption at 1238 cm^{-1} is assigned to C–O–C asymmetric stretching, whereas the signal at 1160 cm^{-1} is assigned to –C–O–C– symmetric stretching. HA NPs are correspondent to bands at 1601, 557 cm^{-1} underlining its presence within biphasic porous structures.

The polymeric component (PCL) was dissolved in dDMSO and THF, and characterized using nuclear magnetic resonance (NMR) and gel permeation chromatography (GPC). The nature of polymeric phase was studied by comparing the NMR spectra of polymer phase obtained from biphasic porous structures and without NPs addition. The correspondence of the signals underlines that CL polymerizes to PCL during porous structures formation (typical ^1H NMR signals in Figure 2d). The average molecular weight of PCL, obtained from GPC analysis (Figure 2e), is around 1600 Da and the distribution of molecular weights 1.6. From this analysis it is evident that the addition of NPs colloidal dispersion during polymerization affects only partially polymerization reaction.

To understand the extent of its impact, we compared the two situations reported in Figure 2e: (i) PCL in biphasic porous

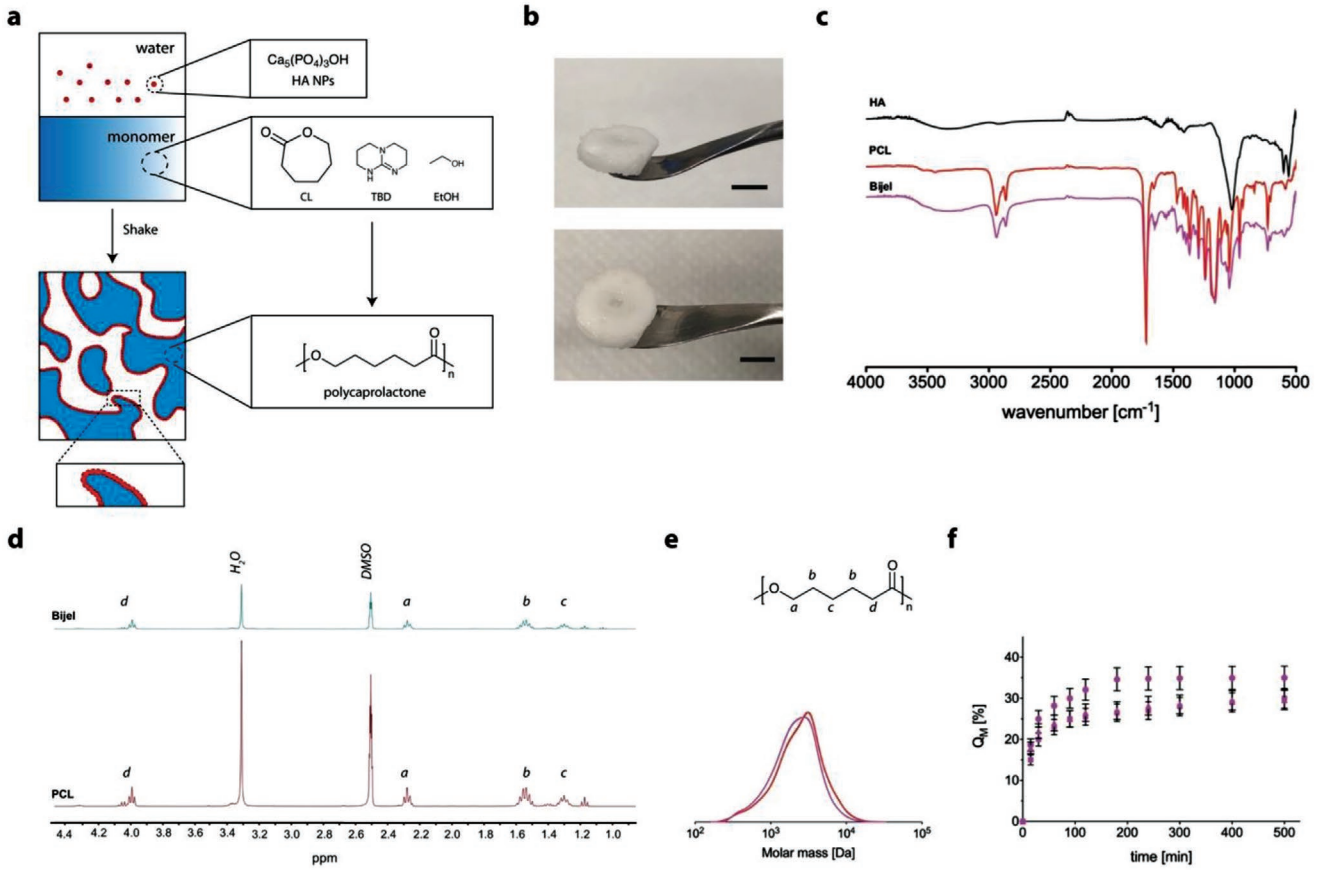

Figure 2. a) Schematic showing the formation of biphasic porous structures formed by the jamming of HA nanoparticle at the oil–water interface. At the beginning oil phase is represented by caprolactone, that is then polymerized into polycaprolactone; b) final aspect of the formed structures (scale bar = 0.5 cm); c) FTIR spectra of HA (black like), PCL (red line), and biphasic porous structures (magenta line); d) ^{1}H-NMR spectra of PCL in biphasic porous structures (red line), without NPs addition (magenta line); e) GPC analysis of PCL in biphasic porous structures (magenta line) and without NPs addition (red line); f) swelling ratio of a biphasic porous structures at acidic pH (squares), neutral pH (triangles) and basic pH (rhombuses) (n = 3, mean ± standard).

structures structure (red line) and (ii) PCL polymerized in the same conditions but without NPs addition (black line). From such observations, it seems that water addition performed at late stages of the test only partially affects the outcome of the polymerization, implying that the meaningful steps in the reaction between the CL monomers and oligomers occur before its addition time. Since the TBD is a catalyst and, as such, is reformed in its original state at the end of the reaction, part of the water interacts with it, deactivating it even at the later stages of the production.

Combining these results, it is possible to state that the key steps of the polymerization occur just at the begging of the shaking and the remaining reaction time is required to let the structure rearrange. Even if the final system cannot be classified as a hydrogel, due to the hydrophobic nature of the polymer used, it presents some similar characteristics. Among them swelling behavior (Figure 2f), biocompatibility and possibility to load drugs or biomolecules (Supporting Information) are in common with the main difference that bijels can also carry and release hydrophobic drugs. Swelling ability, responsible of elastic properties behind hydrogels,[20] is extremely different respect to neat PCL that, as known, is extremely hydrophobic. Our samples indeed present superabsorbent behavior with swelling equilibrium reached, for neutral, acidic, and basic pH, after 1 h (Figure 2f).

Then the biphasic porous nature of the final device was investigated with fluorescent confocal microscopy (**Figure 3** and Supporting Information). In particular the two phases are highlighted using two different dyes in the same sample: rhodamine B (red color) and pyrene (green color). Rhodamine B is water soluble and presents no solubility in caprolactone phase, while pyrene on the contrary is extremely hydrophobic.

In Figure 3a the biphasic structures at different magnifications is visible and verified by the absence of colocalization between the two different dyes used. Similar results were obtained also with other dyes (results in Supporting Information). The two different phases and the interface are well observable in Figure 3b,c: in both these images the black boundary (not colored due to the incompatibility with rhodamine B and pyrene) represents the layer of HA NPs that stabilizes the two immiscible phases. The presence of HA NPs within the network is also underlined by SEM analysis (Figure 3d) with EDS spectra of different region (Figure 3e,f). The absence of colocalization of the signals and the presence of interpenetrating network are typical of biphasic porous structures. The presence of water/oil

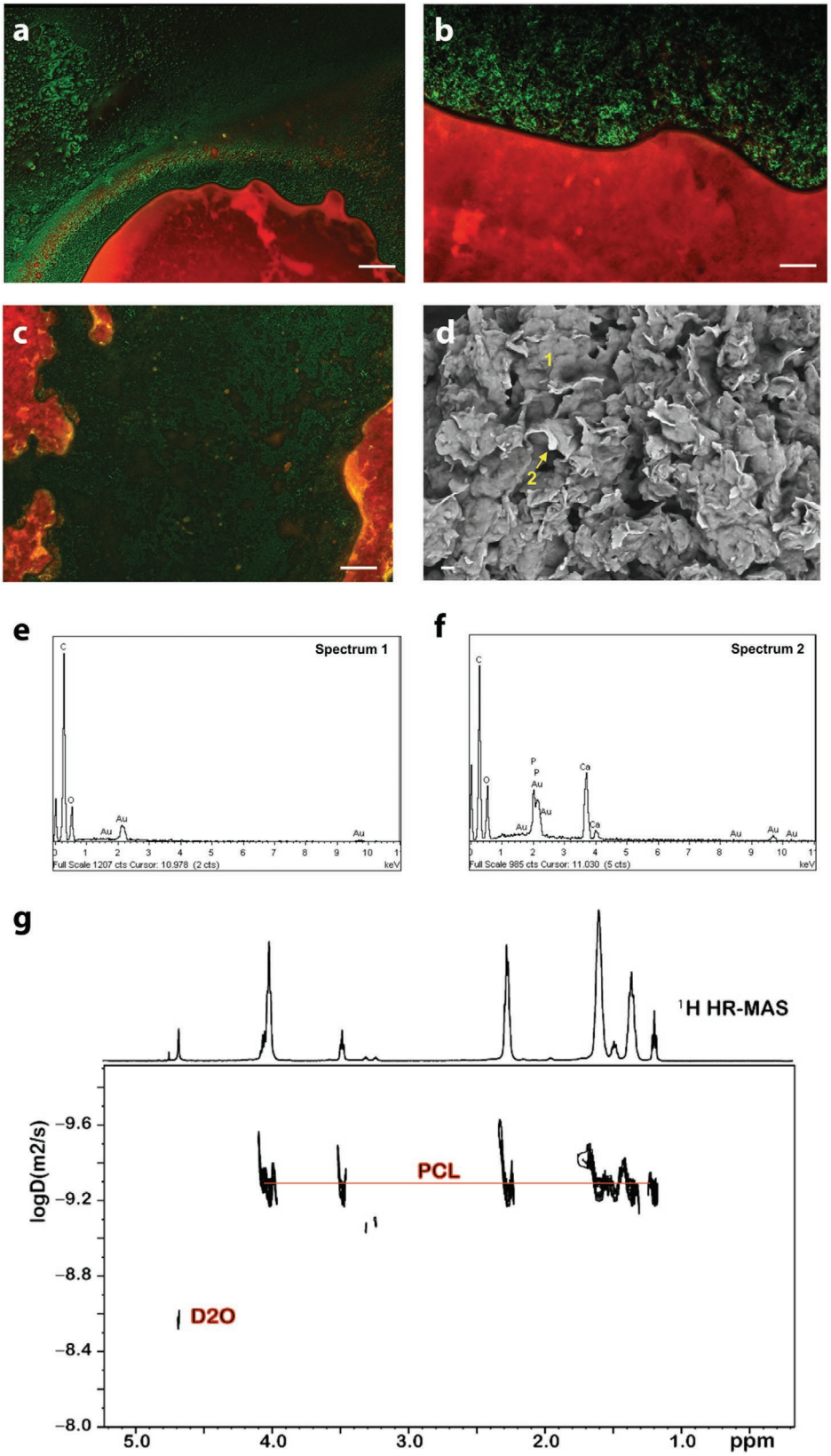

Figure 3. a–c) Confocal fluorescent images of biphasic porous structure with rhodamine B solved in the water phase and pyrene solved in the oil (caprolactone) phase. (scale bar = 100 µm in (a) and 50 µm in (b,c)). d) ESEM images of biphasic porous structure at 1000× magnifications (scale bar = 10 µm). EDS of region 1 e) underlines the presence of PCL, while in region 2 f) the presence of HA is visible. g) ^{1}H HR-MAS DOSY map of the biphasic porous structure sample. The *x*-axis displays the ^{1}H chemical shift (ppm), while the *y*-axis displays the log(*D*) values (m^2 s^{-1}).

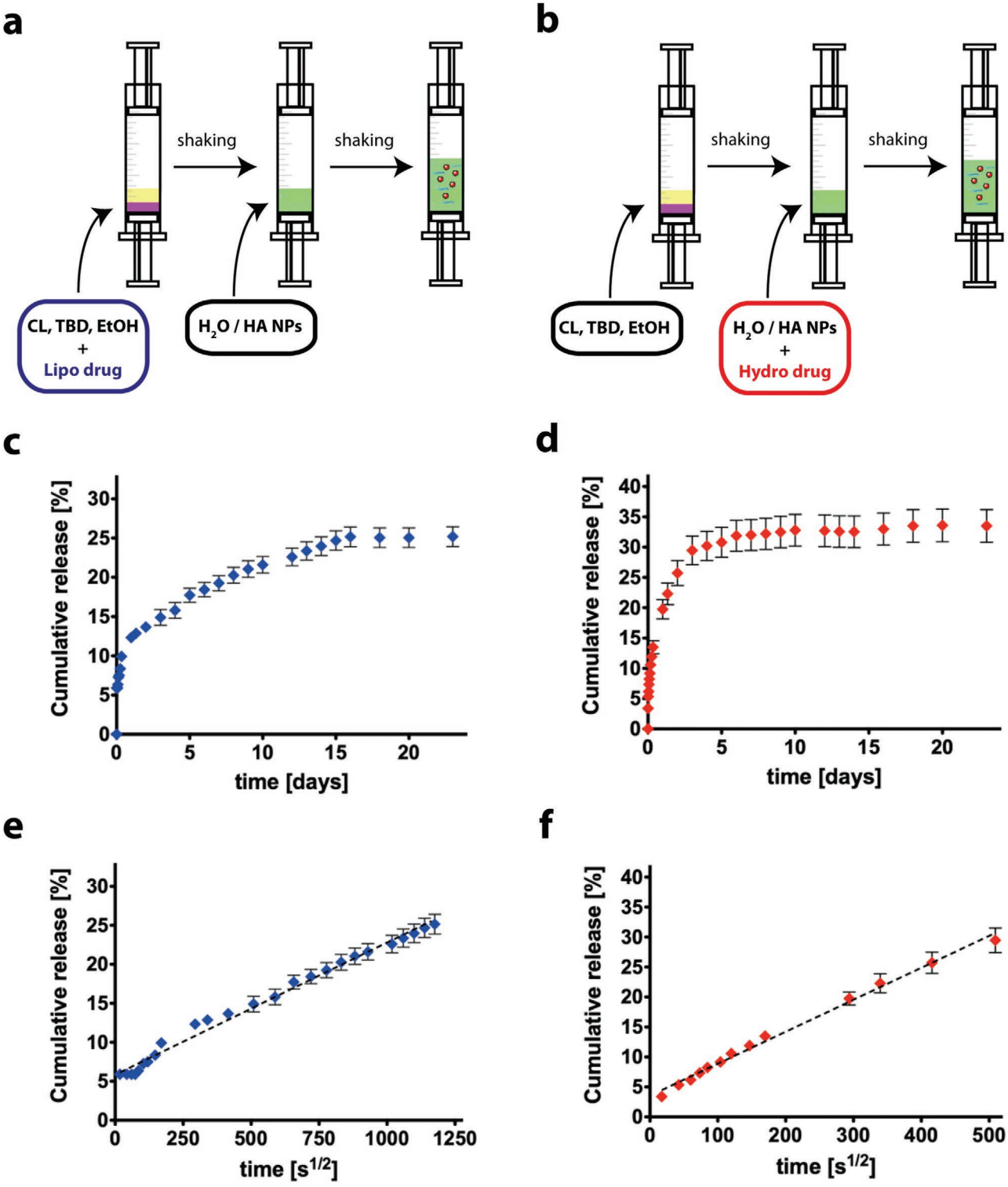

Figure 4. a,b) Loading procedures for hydrophobic and hydrophilic drugs during device formation. c) In vitro release profile of FTIC delivered from biphasic porous structure. d) In vitro release profile of SF delivered from biphasic porous structure. The slope of drug release against the square root of time is representative of Fickian diffusion coefficients for each sample ($p < 0.001$ between all groups). Furthermore, diffusion-controlled release is sustained for 4 d for hydrophilic drug and 15 d for hydrophobic. e,f) Cumulative release (%) is calculated relative to amount of drug loaded ($n = 3$, mean ± standard).

distinct phases is further highlighted by the diffusion-ordered spectroscopy (DOSY) NMR experiments. The DOSY experiment, based on the gradient echo approach, is able to separate different species according to their diffusion coefficient (D). A series of spin echo spectra is measured varying the pulsed field gradient strength, and the signal attenuation is related to the mean

square displacement (MSD) and therefore to the diffusion coefficient of each diffusing species. The resulting DOSY map can be interpreted as a pseudo-2D NMR experiment, with chemical shifts and diffusion coefficients plotted, respectively, along x and y axis.

The DOSY map of our system, reported in Figure 3g, clearly reveals the presence of two distinct diffusing species, ascribed to D_2O with the diffusion coefficient $D_{(D2O)} = 2.6 \times 10^{-9}$ m^2 s^{-1} and to the oil phase (PCL) characterized by a slower diffusion coefficient $D_{(PCL)} = 7.3 \times 10^{-11}$ m^2 s^{-1}. In both cases, the echo attenuation curves show a smooth monoexponential decay. The diffusivity of D_2O in biphasic porous sample is consistent with the literature value of a free diffusion with no barrier experienced by the water molecules.[21]

Moreover, diffusion experiments, performed with variable observation time Δ, show that the MSD of the observed species scales linearly with time Δ (Figure S25, Supporting Information). This indicates that the diffusing molecules undergo unrestricted Gaussian motion and do not experience diffusion barriers or obstacles of the length-scale ≈16 µm accessible by NMR experiments. As said above the main advantage respect to standard hydrogels and standard delivery systems (i.e., micelles, nanoparticles, and others) resides in the possibility to load simultaneously hydrophobic and hydrophilic drugs, able to work as multiple drug delivery systems, in the same device. Hydrophobic drug (here fluorescein isothiocyanate as mimetic, "Lipo drug" in **Figure 4**a) can be loaded in the monomer phase, while hydrophilic drug (sodium fluorescein as drug mimetic, "Hydro drug" in Figure 4b) in the water phase (Figure 4a,b) building a multidrug delivery system.

Loading procedure, during biphasic porous structure formation, allows to load 100% of the drug without affecting the formation of the final structure. Release of hydrophilic and hydrophobic drugs was investigated in vitro under conditions that mimic the in vivo environment using phosphate buffer saline solution. Samples were placed on Petri dishes at 37 °C, and release buffer was replaced with fresh buffer at multiple time points. Data are presented as cumulative drug release, respect to drug loaded, as a function of time. The release of both hydrophobic and hydrophilic drugs are prolonged for more than 20 d (Figure 4c,d). The main difference between them is related to the kinetics. It is indeed visible that the hydrophilic drug presents a quicker kinetics (higher slope vs time) due to the high affinity with the outer aqueous phase. On the contrary hydrophobic drug present a lower affinity with the releasing medium. The drug should be released in a controlled manner to prevent burst release, an unwanted, uncontrolled mechanism commonly visible in hydrogel-based drug delivery system.[4,22] This phenomenon was observed neither for the hydrophobic nor hydrophilic drugs.

After an initial high release, the diffusion-driven trend starts before plateauing. To investigate the difference between hydrophobic and hydrophilic drugs the cumulative drug release was plotted against square root of time ($t^{1/2}$, Figure 4d,f) where a linear relationship indicates Fickian diffusion.[23] Considering the slopes of the linear region it is possible to determine the relative diffusion for each drug through biphasic porous structure observing that they are different. In particular for hydrophilic drug mimetic the slope is steeper and the trend is linear for 4 d while for hydrophobic drug mimetic the slope is flatter and the trend linear for more than 15 d.

This confirms that Fickian diffusion can be maintained for long time for both drug mimetics considered. Indeed even for hydrophilic drug the possibility to maintain linear trend for more than 4 d is extremely important and promising considering that for classic hydrogels the same behavior generally lasts hours.[24] In accordance with drug delivery theory hydrophobic drugs can be release in a more controlled manner due to the solubility in water environment that limit very fast kinetics. Importantly we should notice that both trends are linear, even if drugs used present low steric hindrance so high susceptible to uncontrolled release, overcoming burst and biphasic release mechanisms. Loading drug within this biphasic porous system decreases their release rates, without changing their chemical structure due to the mild loading conditions. This system is so extremely promising to sustain and control the multirelease of drugs with different water affinity. The same results were obtained also for high steric hindrance drug mimetic, that mimic the use of biomolecules or antibodies, and the results are visible in details in the Supporting Information.

3. Conclusions

In conclusion colloidal nanoparticles have been successfully applied to generate biphasic porous structure where the oil phase is characterized by a monomer able to polymerize in bulk condition during structure formation.

We have shown that the advantages of this procedure are: (i) the easy preparation protocol (simply mixing), (ii) the absence of surfactants, (iii) the higher performance due to final polymer phase, and iv) the high versatility due to the presence of oil (monomer) and nanoparticles that can be chosen depending on the final properties and applications considered. This is an essential first step in formulating them for many different industrial and medical applications, specifically due to their promising results as multiple drug delivery systems.

4. Experimental Section

The experimental section is available in the Supporting Information.

Supporting Information

Supporting Information is available from the Wiley Online Library or from the author.

Acknowledgements

F.P. and A.R. share the first authorship. All authors would like to thank Oystein Ovrebo for proof reading and fruitful discussion.

Open access funding provided by Politecnico di Milano within the CRUI-CARE Agreement.

Conflict of Interest

The authors declare no conflict of interest.

Data Availability Statement

Data available on request from the authors.

Keywords

bijels, drug delivery, hydroxyapatite, mixture of polymers, polymerization

Received: June 14, 2021
Revised: August 3, 2021
Published online:

[1] C. L. Huang, J. Forth, W. Y. Wang, K. L. Hong, G. S. Smith, B. A. Helms, T. P. Russell, *Nat. Nanotechnol.* **2017**, *12*, 1060.
[2] E. Koos, N. Willenbacher, *Science* **2011**, *331*, 897.
[3] a) A. J. Krzysko, E. Nakouzi, X. Zhang, T. R. Graham, K. M. Rosso, G. K. Schenter, J. Ilavsky, I. Kuzmenko, M. G. Frith, C. F. Ivory, S. B. Clark, J. S. Weston, K. M. Weigandt, J. J. De Yoreo, J. Chun, L. M. Anovitz, *J. Colloid Interface Sci.* **2020**, *576*, 47; b) J. Tang, P. J. Quinlan, K. C. Tam, *Soft Matter* **2015**, *11*, 3512; c) E. C. Giakoumatos, A. Aloi, I. K. Voets, *Nano Lett.* **2020**, *20*, 4837; d) R. J. Archer, A. J. Parnell, A. I. Campbell, J. R. Howse, S. J. Ebbens, *Adv. Sci.* **2018**, *5*, 1700528.
[4] S. Bernhard, M. W. Tibbitt, *Adv. Drug Delivery Rev.* **2021**, *171*, 240.
[5] a) F. Jansen, J. Harting, *Phys. Rev. E* **2011**, *83*, 046707; b) E. M. Herzig, K. A. White, A. B. Schofield, W. C. K. Poon, P. S. Clegg, *Nat. Mater.* **2007**, *6*, 966.
[6] M. E. Cates, P. S. Clegg, *Soft Matter* **2008**, *4*, 2132.
[7] a) K. A. White, A. B. Schofield, P. Wormald, J. W. Tavacoli, B. P. Binks, P. S. Clegg, *J. Colloid Interface Sci.* **2011**, *359*, 126; b) M. Reeves, A. T. Brown, A. B. Schofield, M. E. Cates, J. H. J. Thijssen, *Phys. Rev. E* **2015**, *92*, 032308.
[8] M. F. Haase, K. J. Stebe, D. Lee, *Adv. Mater.* **2015**, *27*, 7065.
[9] a) D. Y. Cai, P. S. Clegg, *Chem. Commun.* **2015**, *51*, 16984; b) K. A. Rumble, J. H. J. Thijssen, A. B. Schofield, P. S. Clegg, *Soft Matter* **2016**, *12*, 4375.
[10] J. Wu, G. H. Ma, *Small* **2016**, *12*, 4633.
[11] a) K. Stratford, R. Adhikari, I. Pagonabarraga, J. C. Desplat, M. E. Cates, *Science* **2005**, *309*, 2198; b) T. J. Thorson, E. L. Botvinick, A. Mohraz, *ACS Biomater. Sci. Eng.* **2018**, *4*, 587; c) J. A. Witt, D. R. Mumm, A. Mohraz, *J. Mater. Chem. A* **2016**, *4*, 1000.
[12] S. Gadde, *MedChemComm* **2015**, *6*, 1916.
[13] a) D. Placente, L. A. Benedini, M. Baldini, J. A. Laiuppa, G. E. Santillan, P. V. Messina, *Int. J. Pharm.* **2018**, *548*, 559; b) I. Vismara, S. Papa, V. Veneruso, E. Mauri, A. Mariani, M. De Paola, R. Affatato, A. Rossetti, M. Sponchioni, D. Moscatelli, A. Sacchetti, F. Rossi, G. Forloni, P. Veglianese, *ACS Nano* **2020**, *14*, 360; c) B. H. Jones, T. P. Lodge, *ACS Nano* **2011**, *5*, 8914.
[14] a) G. Perale, F. Rossi, M. Santoro, M. Peviani, S. Papa, D. Llupi, P. Torriani, E. Micotti, S. Previdi, L. Cervo, E. Sundstrom, A. R. Boccaccini, M. Masi, G. Forloni, P. Veglianese, *J. Controlled Release* **2012**, *159*, 271; b) X. G. Wang, L. Xu, M. J. Li, X. Z. Zhang, *Angew. Chem., Int. Ed.* **2020**, *59*, 18078.
[15] X. Yao, J. Mu, L. Zeng, J. Lin, Z. Nie, X. Jiang, P. Huang, *Mater. Horiz.* **2019**, *6*, 846.
[16] a) A. M. Sisso, M. O. Boit, C. A. DeForest, *J. Biomed. Mater. Res., Part A* **2020**, *108*, 1112; b) W. Deng, H. Yamaguchu, Y. Takashima, A. Harada, *Angew. Chem., Int. Ed.* **2007**, *46*, 5144.
[17] a) C. Weber, S. Morsbach, K. Landfester, *Angew. Chem., Int. Ed.* **2019**, *58*, 12787; b) J. Feijen, W. E. Hennink, Z. Y. Zhong, *Nanomedicine (London, UK)* **2013**, *8*, 177; c) K. Riehemann, S. W. Schneider, T. A. Luger, B. Godin, M. Ferrari, H. Fuchs, *Angew. Chem., Int. Ed.* **2009**, *48*, 872.
[18] M. F. Haase, N. Sharifi-Mood, D. Lee, K. J. Stebe, *ACS Nano* **2016**, *10*, 6338.
[19] W. N. Ottou, H. Sardon, D. Mecerreyes, J. Vignolle, D. Taton, *Prog. Polym. Sci.* **2016**, *56*, 64.
[20] a) K. Hoshino, T. Nakajima, T. Matsuda, T. Sakai, J. P. Gong, *Soft Matter* **2018**, *14*, 9693; b) A. M. Kloxin, M. W. Tibbitt, K. S. Anseth, *Nat. Protoc.* **2010**, *5*, 1867; c) C. Yang, M. W. Tibbitt, L. Basta, K. S. Anseth, *Nat. Mater.* **2014**, *13*, 645.
[21] M. Holz, S. R. Heil, A. Sacco, *Phys. Chem. Chem. Phys.* **2000**, *2*, 4740.
[22] a) J. Y. Li, D. J. Mooney, *Nat. Rev. Mater.* **2016**, *1*, 16071; b) J. Yoo, Y. Y. Won, *ACS Biomater. Sci. Eng.* **2020**, *6*, 6053; c) P. Makvandi, U. Josic, M. Delfi, F. Pinelli, V. Jahed, E. Kaya, M. Ashrafizadeh, A. Zarepour, F. Rossi, A. Zarrabi, T. Agarwal, E. N. Zare, M. Ghomi, T. K. Maiti, L. Breschi, F. R. Tay, *Adv. Sci.* **2021**, *1*, 2004014.
[23] a) K. Vulic, M. M. Pakulska, R. Sonthalia, A. Ramachandran, M. S. Shoichet, *J. Controlled Release* **2015**, *197*, 69; b) K. Vulic, M. S. Shoichet, *J. Am. Chem. Soc.* **2012**, *134*, 882.
[24] a) T. R. Hoare, D. S. Kohane, *Polymer* **2008**, *49*, 1993; b) E. Mauri, G. Perale, F. Rossi, *ACS Appl. Nano Mater.* **2018**, *1*, 6525.